ATLAS Internal Note
INDET-NO-036
3 February 1994

Radiation Resistans of $GaAs$ Structures Based on $\pi-\nu$ Junction.

Chmill V.B., Chuntonov A.V., Krupnyi G.I., Rastsvetalov Ya.N.,
Stetcenko G.N., Vorobiev A.P., Yanovich A.A.

Institute for High Energy Physics, Protvino, Russia.

Khludkov S.S., Koretski A.A., Potapov A.I., Tolbanov O.P.

Siberian Institute for Physics and Technology, Tomsk, Russia.

Abstract :

The results of studying $GaAs$ samples with build-in π–ν junction as the base for the construction of the radiation resistant coordinate sensitive detectors are presented. The $GaAs$ samples have been exposed to the IHEP beam of the linear proton accelerator, using Al target for neutron production. The $I-V$–characteristics of $GaAs$ samples have been analyzed to search for the charge of its properties. The study of the radiation resistance of the $GaAs$ samples has shown that their main characteristics (charge collection efficiency, signal/noise ratio) degrade less than 20% at the integral neutron fluence of $1.2 \cdot 10^{15}$ cm^{-2}.

Introduction

There are very demanding requirements on the radiation resistance of apparatus for use at the new, high luminosity colliders (LHC,SSC,UNK,VLEPP). For example, at the LHC luminosity of $10^{34} cm^{-2} s^{-1}$, in the region of a microvertex detector we can expect a neutron fluence of around $10^{14} n/cm^2$ and a dose of absorbed electromagnetic radiation of approximately 10 MRad per year of operation [1].

Here we present the results of experimental investigations of the effect of very large neutron fluences ($10^{15} n/cm^2$) on the characteristics of GaAs detector structures with "built-in" $\pi - \nu$-junctions. The sensitivity of this type of structure to ionising radiation has been reported previously in references [2-4], where they have been considered as a basis for the fabrication of microstrip coordinate-sensitive detectors. The degradation of the GaAs structures has been measured in terms of the reduction in charge collection efficiency and signal/noise ratio measured for minimum ionising beta particles from a radioactive (^{106}Ru) source and from changes in I-V and C-V electrical characteristics.

Samples of GaAs $n^+ - \pi - \nu - n$ structures have also been exposed to gamma rays from a ^{137}Cs source at a dose rate of 6.074 rad/sec. These results are reported in reference [3].

1 Description of Investigated Structures and of Experimental Method

For these investigations of the radiation resistance of $p - \pi - \nu - n$ GaAs structures, high resistivity layers were prepared either by liquid-phase epitaxial growth or by diffusion doping of semi-insulating substrate material with iron or chromium as a compensating dopant. Low resistivity n-type GaAs substrates were used for mechanical support. This material was prepared in the Siberian Institute for Physics and Technology,Tomsk, by the Bridgman method of crystal growth in a magnetic field.The high resistivity layers have been prepaered by liquid - phase epitaxial growth doping of substrate material with iron. Commercial low resistivity n-type samples, prepared using the Czochralski method, were also used for comparison. For fabrication of high resistivity layers in this material, compensation was achieved by in-diffusion of chromium as a dopant. Neutron irradiation of the samples prepared was carried out at the I-100 proton linear accelerator laboratory of the Institute for High Energy Physics,using the standard target of total absorption length of aluminium. The characteristics of the proton beam from the accelerator are given in Table 1.

Parameter	Value
Energy	100 MeV
Beam current	50 mA
Pulse length	100 μs
Frequency	0.5 Hz

Table 1: *Parameters of the I-100 proton beam. The beam size and its transverse shape (circular or elliptical) depends on the tuning of the accelerator and varies from 5 to 50 cm^2. The beam is made up of 0.6 ns bunches at 6 ns intervals.*

For the irradiation of the samples, a target of aluminium of total absorption length for the 100 MeV protons was used. The GaAs samples to be irradiated were located on the beam axis at a distance of 0.1 m from the target. The main characteristics of the radiation at this point are given in Table 2. The neutron dose was accumulated by the GaAs samples at a rate of $(4 - 5)10^{12} n/cm^2$per hour. A detailed description of the

system used for monitoring the beam, experimental volume and detector characteristics will be given elsewhere. Four samples were exposed to neutron irradiation - two commercial samples and two fabricated in Tomsk laboratory. In order to simulate more faithfully the actual conditions to be expected in practical use of the detectors, one sample of each type was irradiated under a reverse bias voltage of 300V, since at an electric field of more than 1V/micron of thickness, defect migration mechanisms and formation of more complex defects become more significant [9].

Average neutron energy MeV	Neutron fluence $E_n > 6MeV$	Gamma dose Rad/proton	Absorbed dose(Rad) 20 min. after beam off
23 ± 3	$(1.2 \pm 0.2) \times 10^{-4}$	$(4.7 \pm 0.9) \times 10^{-13}$	(1.2 ± 0.4)

Table 2: *Main Characteristics of the Irradiation Volume. The absorbed dose for the typical time after beam switch off up to sample extraction time. The exposure was typically two or more hours.*

The irradiation was carried out in stages, with the response of the samples to beta particles from a ^{106}Ru source being checked at each stage.

2 Influence of Irradiation-induced defects on the electro-physical properties of the test structures

The present understanding of radiation-induced defects in low resistivity GaAs crystals is reviewed in references [5-8]. When low resistance GaAs samples are exposed to high energy ionising radiation [5], compensation of the electrical conductivity has been demonstrated. This compensation is found not to depend on either the type of the initial conductivity or on single impurities, but does depend on the trapping of free charge carriers by radiation-induced defects.

Figure 1 shows the change in resistivity of GaAs samples subjected to irradiation by fast protons, neutrons and electrons [10]. The resistivity tends to a limiting value of $10^9 ohmcm$ independently of the type of irradiating particle. The increase in specific resistance is due mainly to the reduction in the density of free charge carriers. In our case, the initial compensation means that there is no further increase in specific resistance up to some limit of the neutron dose from the I-100 accelerator. For our samples of GaAs which have been compensated by iron, the typical resistance only begins to show an increase for neutron fluences in excess of $10^{15} n/cm^2$ (Fig.1). The I-V characteristic variation with neutron irradiation was studied using $\pi - \nu - n$ structures. The forward I-V characteristic is illustrated in Figure 2. An ohmic part to the characteristic can be observed for both forward and reverse bias voltages of less than 0.1V (I). The minority carrier lifetime, τ_0, in the space charge region (SCR) has been measured from the slope of this part of the I-V curve. The measured value of τ_0 is found to be independent of the irradiation and lies in the range $(5-9)10^{-10} s$. The recombination part of the forward characteristic (II) changes significantly. When the dose increases, it is observed that this part tends to disappear, i.e. recombination in the SCR region becomes negligible in spite of the widening of this area of the volume charge. The third part (III), connected with the double injection of current in the π layer, has also changed: with increased dose this part of the current becomes smaller and, in the limit, we see the transformation to an ohmic state (Fig.2). Estimation shows that when the dose increases, the specific resistance of the thin π-layer also grows in proportion up to 10^8 ohmcm (Fig.4). Regions II and III of the reverse bias branch

also become deformed (Fig.3). If we take into account the expression for the width of the depletion region, we have,

$$j_g \sim (\tau_0^2(N_d - N_t))^{-1/2}$$

which shows that the generation current is inversely proportional to the product of the minority carrier lifetime and the square root of the net dopant concentration, (other values being held constant). However, it was established that the minority carrier lifetime in the sensitive region did not depend on the radiation dose, and the dependence on the dopant concentration was weaker than expected.

Let us analyse the processes in the π-layer. There is a sharp increase in the resistance of the π-layer, as shown in Figure 4. A classical conductivity-modulation method was used to establish the lifetime of the minority carriers (electrons) in the π-layer. A fixed-length forward biased rectangular pulse was applied to the structure, resulting in the injection of electrons into the π-region from the displaced $\pi - \nu$ junction. In the fixed time interval the testing rectangular pulse was applied to the structure again. Because there is no field in the π - layer the shape of the output pulse shows the recovery of the $\pi - \nu$ region after the injecting pulse. The minority carriers were washed out due to recombination only. When the fluence of neutrons increased the lifetime decreased from $10^{-4} to 10^{-10} sec.$ At a neutron fluence higher than $10^{14} - 10^{15} n/cm^2$ it was impossible to create injection of electrons into the π-region.Evidently the reason for this phenomenon is the very high resistance of this region and the weak injection of the $\pi - \nu$ junction. All these results are in good agreement with the model,where we can consider our structure as a chain two connected resistors of the $\pi - \nu$ junction and of the π-region. Due to the influence of the absorbed neutrons, the additional compensation of the π and ν regions can be observed. The resistance of the π -region increases, (as seen in Figure 4), but the $\pi - \nu$ junction is washed out. As a result, at a limiting dose of $10^{15} n/cm^2$ a typical *p-i-n* structure develops. The same conclusion can be obtained from C-V variations, (cf. the region of the forward step in Figure 6), and from the sharp decrease of the photovoltaic e.m.f. with increased radiation dose (Figure 5). This is because charge carriers created by absorption of light cannot be effectively separated by the field of the SCR. Such a model easily explains the high radiation resistance of the $\pi - \nu - n$ structures doped with iron because of the higher initial level of doping and much lower resistance of the π layer.

GaAs samples of $n^+ - \pi - \nu - n$ structures have also been irradiated using the U-70 accelerator, with a fluence of neutrons around $10^{17} n/cm^2$. After irradiation the structure became like a pure *p-i-n* type. This can be confirmed by the changing of the forward I-V characteristic. The growth of the resistance in the forward region can be seen in these I-V characteristics which are typical of *p-i-n* structures. At the same time, the response of the structures to beta particles from a Ru^{106} source completely disappears even at near-breakdown bias voltages. The specific resistance of the i-region reached $10^9 ohmcm$. This result confirms the earlier conclusion that a peculiarity of highly irradiated samples of GaAs is i-type conductivity independently of the type of conductivity of the inital material [9].

3 Results of investigation of sensitivity of GaAs structures to minimum ionising beta particles.

Figures 7-9 show the measured pulse height spectra from structures which had no bias voltage applied during the irradiation. Figures 10-12 show the data for samples which were biased to 300V during the radiation. It was not possible to estimate the influence of the bias voltage on the rate of degradation of the structures because of the small number of structures investigated during the experiment, but in each case GaAs structures which were chromium compensated degraded much earlier: neutron fluences of $4 \times 10^{14} n/cm^2$ led to results similar to those for $1.0 - 1.2 \times 10^{15} n/cm^2$ for samples doped with iron. The deterioration in S/N ratio due to the irradiation was not more than 20% for the latter. The much lower radiation resistance of chromium doped samples can be explained by the following. To decrease the specific capacity of these structures (which leads to an increase in the S/N ratio for samples before irradiation (Fig.12)), the sample processing used a chromium concentration which was ten times less than that of the iron in the case of doping by the latter. It is well known that radiation-induced defects in GaAs give deep trapping centres which have compensating properties like iron and chromium. Consequently a higher concentration of the chromium or iron dopants at higher values of neutron fluence will have a correspondingly greater influence relative to that of the radiative traps. One of the properties of GaAs after irradiation is the decrease in the intensity of radiative recombination, [5-9], pointing to the predominant creation of non-radiative recombination centres. Significant distortion of the lattice near the radiation-induced defects leads to an increase of the probability of multi-phonon non-radiative recombination of charge carriers and distortion of the lattice is also at the origin of recombination-stimulated migration of defects, [10]. All of these lead to a decrease of the lifetime of a non-equilibrium concentration of charge carriers in $\pi-$ and $\nu-$ layers caused by ionisation by beta particles. For neutron fluences $> 10^{15} n/cm^2$ full charge collection requires an increase of the electric field in the structure so that the charge collection time is not longer than the lifetime of non-equilibrium charge carriers (figs. 8 and 11). As discussed in Section 2, during the neutron beam irradiation of GaAs, additional compensation of the semiconductor takes place, leading to an increase in the specific resistance of the $\pi and \nu$ layers of the structure. The specific resistance of the π region can be approximately ten times that of other layers. It is supposed that the extension of the SCR with increasing reverse bias voltage will take place mainly in the ν-region but with the increase of the specific resistance of the π region, the voltage decrease does not occur over the whole sensitive thickness of the sample. To create the required electric field inside the whole sensitive region of the sample, it is necessary to raise the bias voltage [4]. This change of the voltage distribution between $\pi and \nu$ layers together with the decreased lifetime of non-equilibrium charge carriers leads to the observed degradation of the sample response to beta particles.

4 Conclusion

GaAs structures based on commercial low resistivity materials with increased chromium doping concentration can be created in principle. It can be expected that the radiation resistance of such structures will be similar to that of similar structures compensated by iron. The present results confirm the possibility of the use of such structures as a basis for the fabrication of radiation-resistant coordinate-sensitive structures.

References

[1] Ferrari A. et. al. // EAGLE Internal Note, CAL-NO-005, Nov. 1991.

[2] Vorobiev A.P. et. al. // IHEP Preprint 91-192 Protvino, 1991 (in Russian).

[3] Chmill V.B. et. al. // Nucl. Instr. and Meth. 1993, V.A326, p.310.

[4] Vorobiev A.P. et. al. // IHEP Preprint 92-168 Protvino, 1992 (in Russian), be published in NIM.

[5] Aukerman L.W. Semicond and Semimetals V.4 / ed. R.K. Willardson and A.C. Beer (N.Y.Acodemic Press, 1968).

[6] Coates R. and Mitchel E.W.J. // Adv. Physics, 1975, V.24, p.593.

[7] Lang D.V. // Inst. Phys. Conf. Ser. 1977, n31, p.70.

[8] Brudnyi V.N. et. al. // Solid State Comm. Vol.34 pp.117-119, Pergamon Press Ltd. 1980.

[9] Jeong M.U. et. al. // Rad. Eff. in Semicond. Gordon and Breac Publish. N.Y.,p.287, 1971.

[10] Brudnyi V.N, Krivov M.A. // Radiations Damage in Gallium Arsenide. Izvestia VUZ. N1(212), 1980.

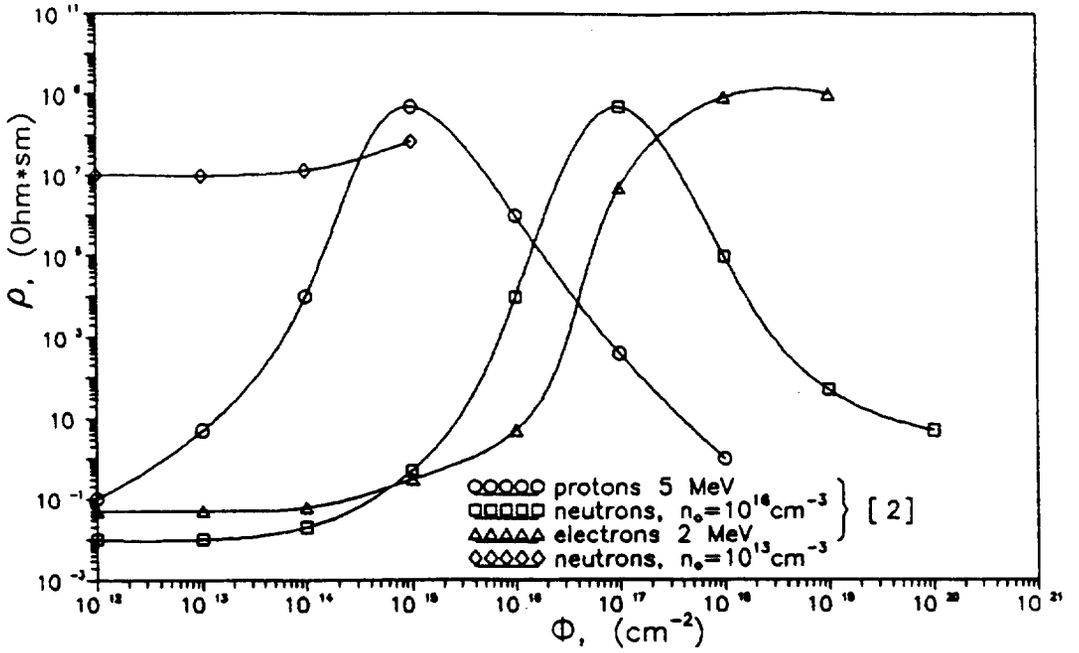
ρ, (Ohm*sm)
Φ, (cm⁻²)
protons 5 MeV
neutrons, n₀=10¹⁶cm⁻³
electrons 2 MeV
neutrons, n₀=10¹³cm⁻³
[2]

Fig 1

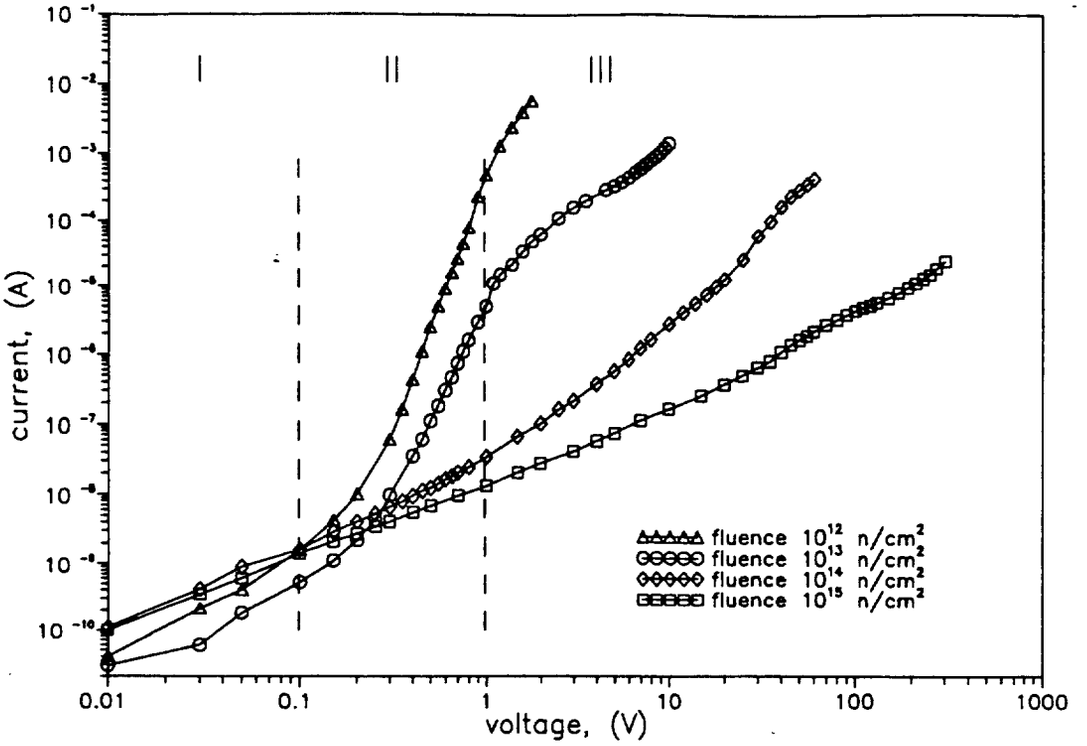
I
II
III
current, (A)
voltage, (V)
fluence 10^{12} n/cm^2
fluence 10^{13} n/cm^2
fluence 10^{14} n/cm^2
fluence 10^{15} n/cm^2

Fig 2

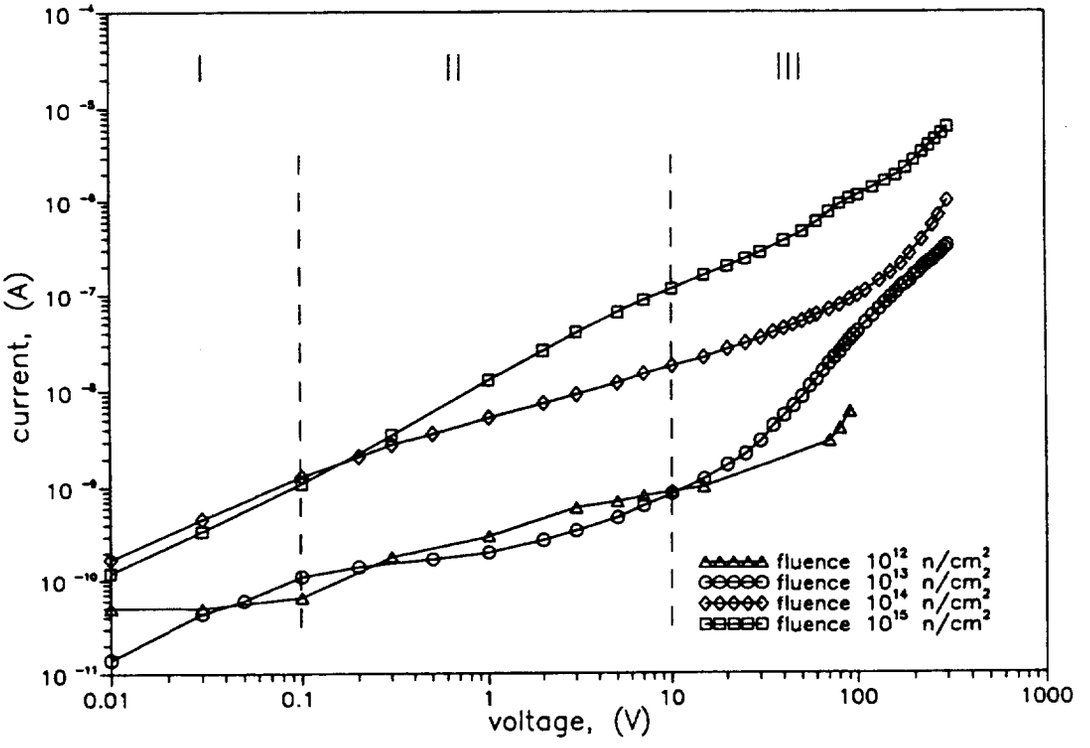
I
II
III
current, (A)
voltage, (V)
fluence 10^{12} n/cm^2
fluence 10^{13} n/cm^2
fluence 10^{14} n/cm^2
fluence 10^{15} n/cm^2

Fig 3

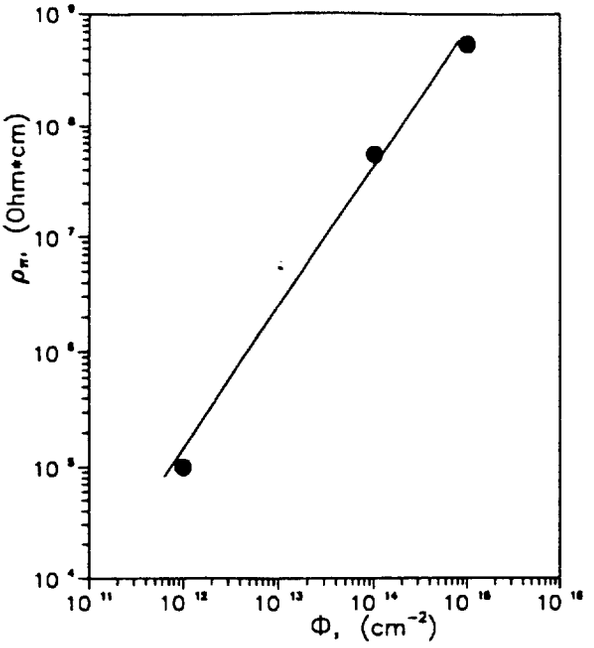

Fig 4

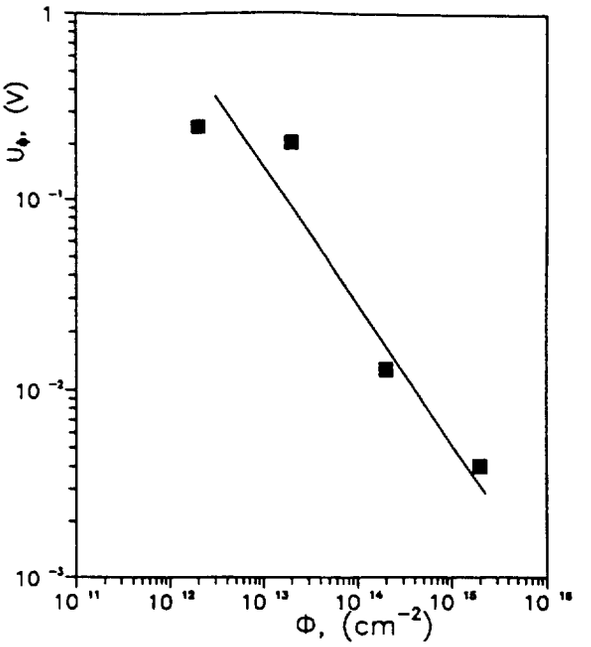

Fig 5

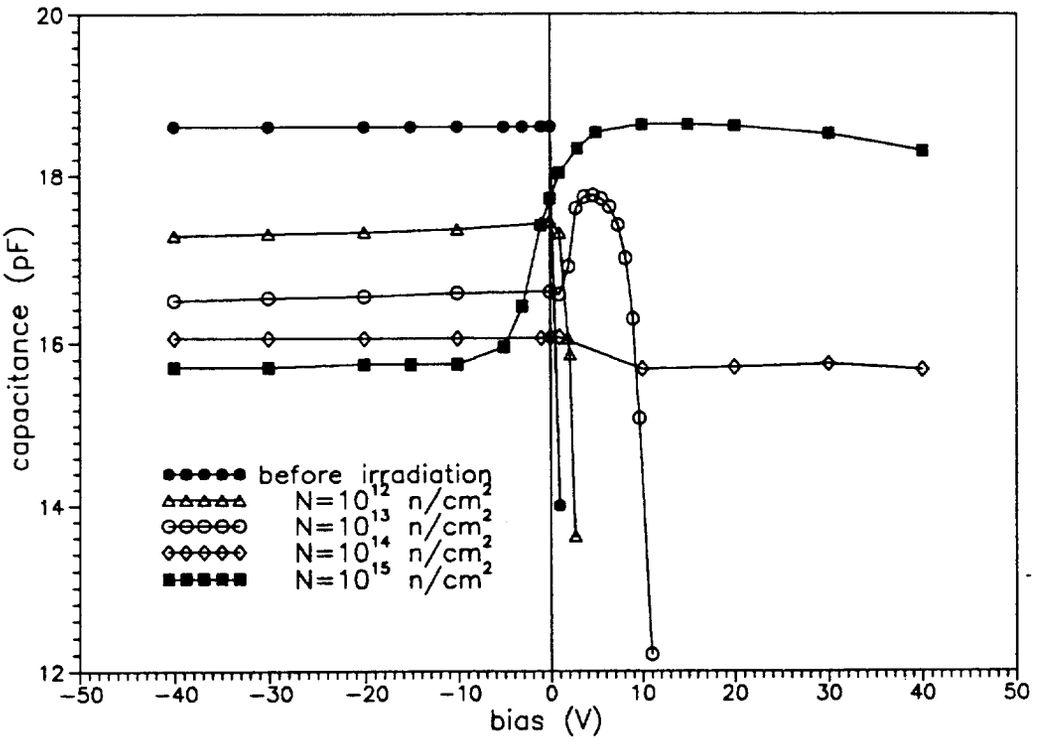

Fig 6

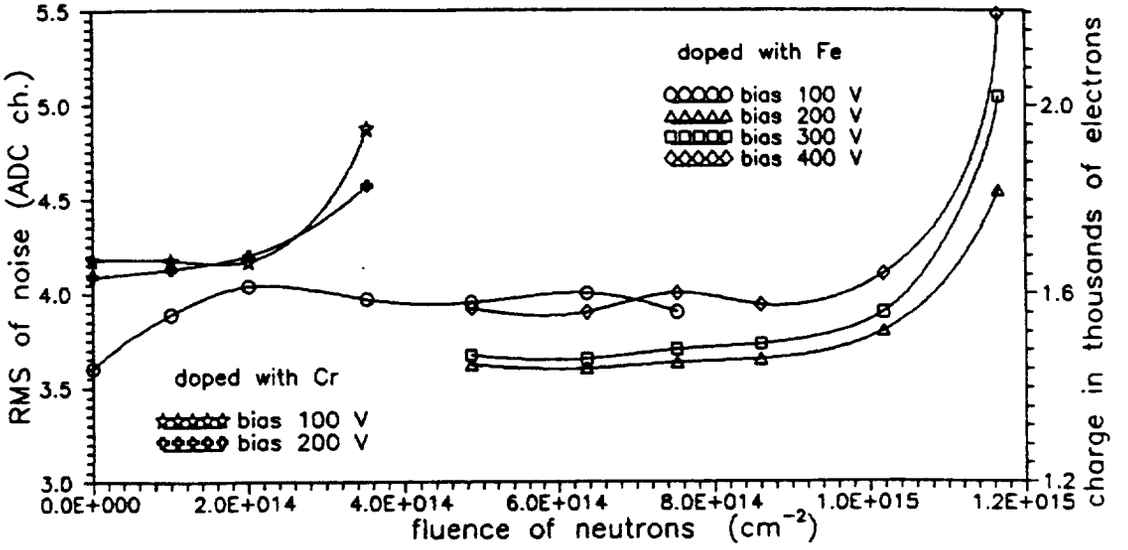

Fig. 7

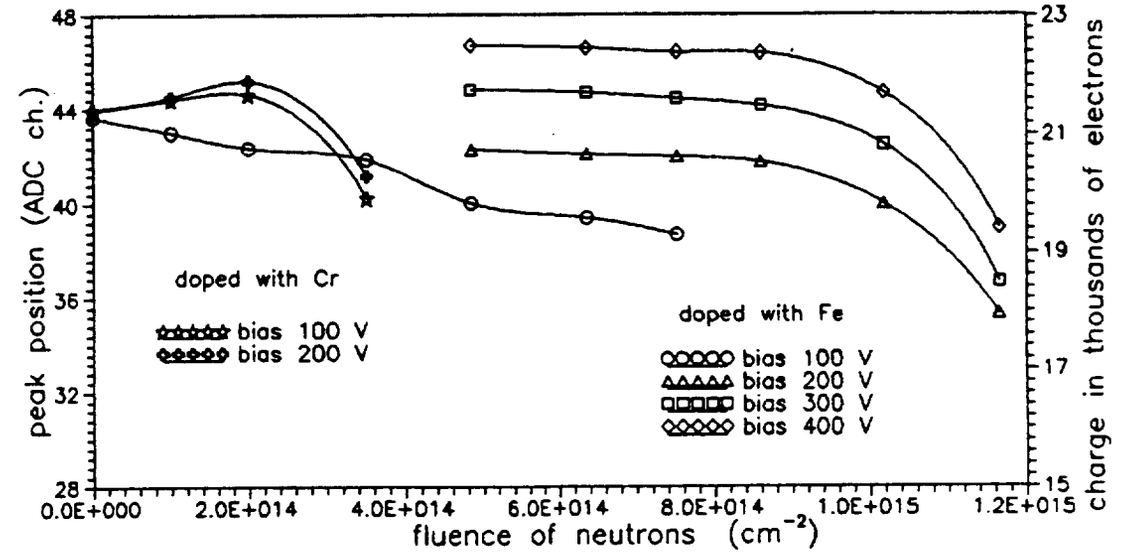

Fig. 8

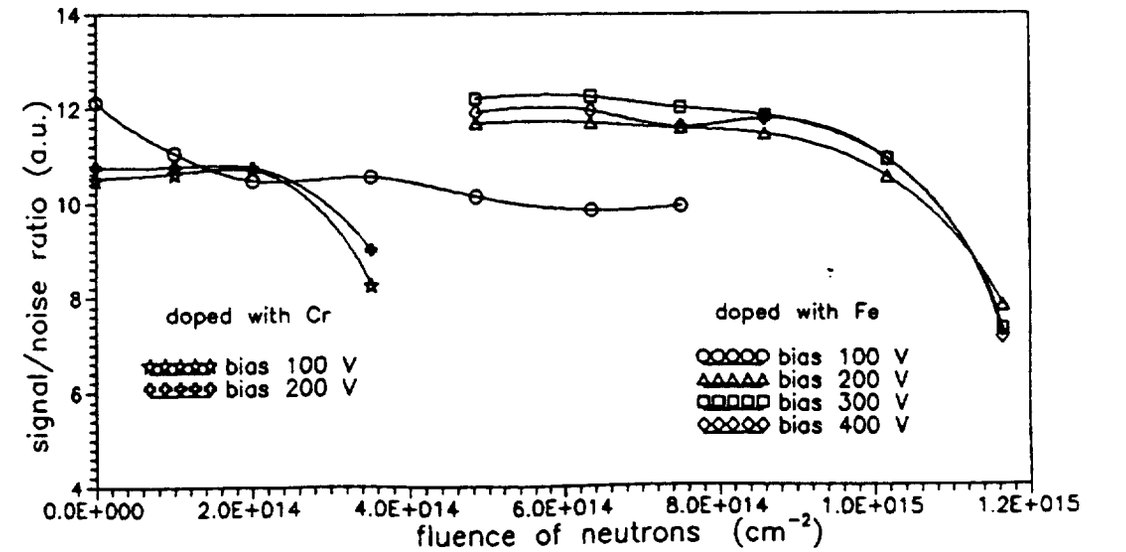

Fig 9

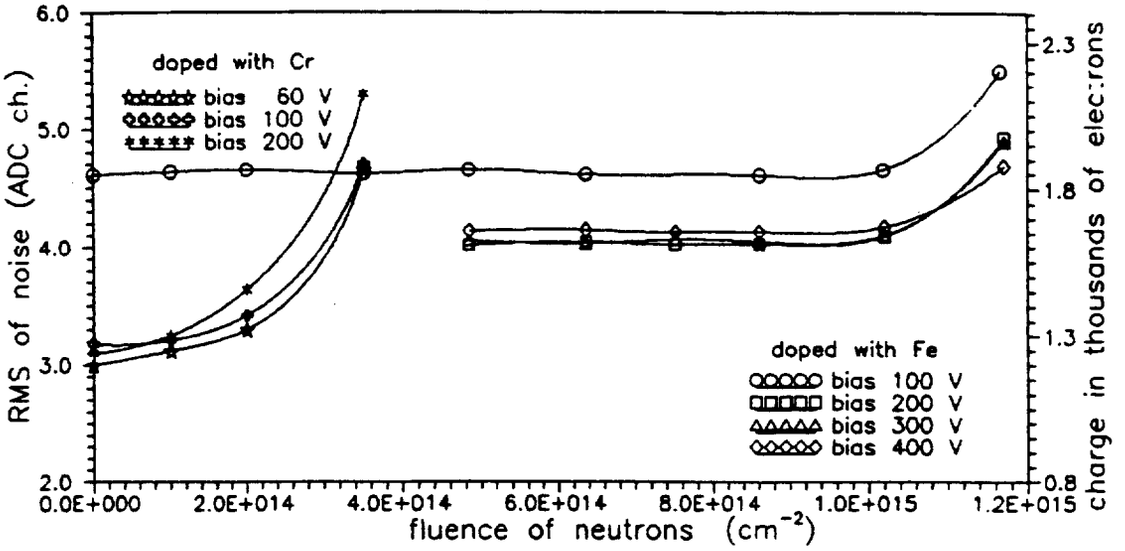

Fig 10

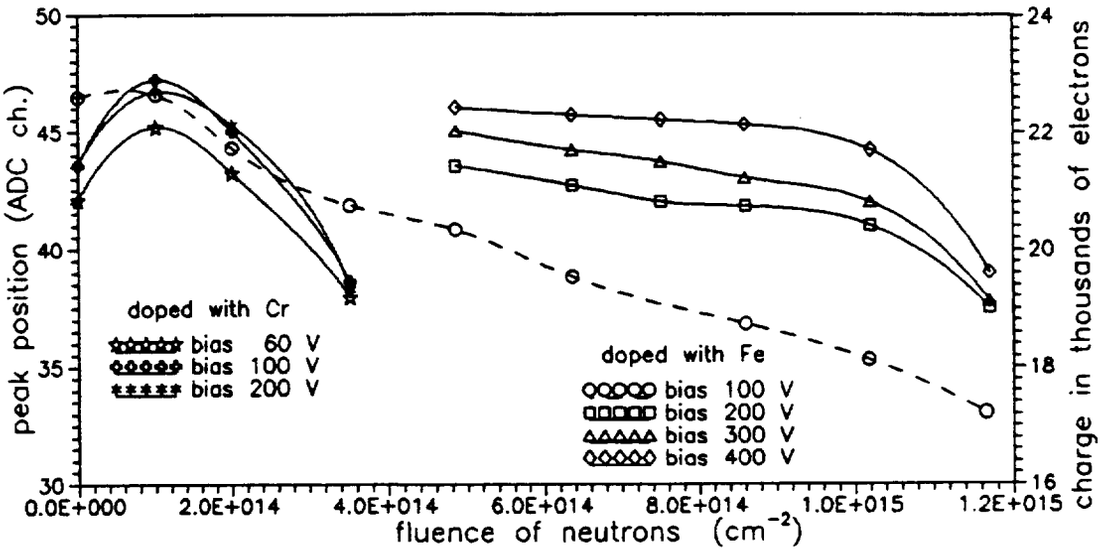

Fig 11

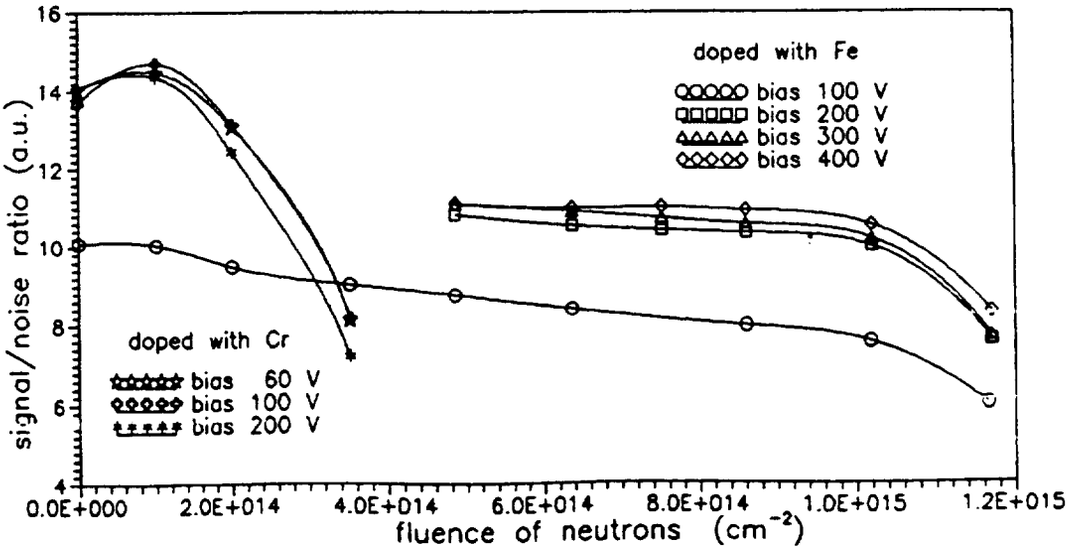

Fig 12